Hierarchical highway recognition from satellite images

M. Haindl, A. Gagalowicz, B. Jedynak

Computer Science/Department of Interactive Systems

Report CS-R9356 December 1993

CWI is the National Research Institute for Mathematics and Computer Science. CWI is part of the Stichting Mathematisch Centrum (SMC), the Dutch foundation for promotion of mathematics and computer science and their applications.
SMC is sponsored by the Netherlands Organization for Scientific Research (NWO). CWI is a member of ERCIM, the European Research Consortium for Informatics and Mathematics.

P.O. Box 94079, 1090 GB Amsterdam (NL)
Kruislaan 413, 1098 SJ Amsterdam (NL)
Telephone +31 20 592 9333
Telefax +31 20 592 4199

Hierarchical Highway Recognition from Satellite Images

Michal Haindl
CWI
P.O. Box 94079, 1090 GB Amsterdam, The Netherlands
mh@cwi.nl

Andre Gagalowicz, Bruno Jedynak
Institut National de Recherche
B.P. 105 -78153, Rocquencourt, France
ag@bora.inria.fr, jedynak@bora.inria.fr

Abstract

We present an algorithm for multiscale highway recognition from high resolution panchromatic satellite data. Proposed filters first detect possible highway elements on an image. Data compression and subsequent rough scale optimization yields a rough scale highway estimation which serves as a basis for precise location of a highway in the original resolution scale in the last step of the algorithm.

AMS Subject Classification (1991): 68T10, 68U10
CR Subject Classification (1991): I.5.4, I.4.8
Keywords & Phrases: highway recognition, satellite images
Note: This paper was presented on the 8th SCIA Conference in Tromso, 1993.

1. Introduction

Recognition of a highway in a high resolution image is a simple task for a human observer, but automatic detection is complicated by the statistical similarity of road and off-road elements. Several algorithms have been proposed to detect road or similar linear elements (i.e. runways [6] or rivers [5]) from remote sensing data. Fischler, Tanenbaum, and Wolf [4] describe a method where locally evaluated road evidence from multiple sources is combined, followed by global optimization using either a graph search or dynamic programming technique. Zhu and Yeh [12] present a method for road network detection where edge detection is used to detect antiparallel pairs of segments. These segments are used as seeds in generating longer road pieces through the use of road growing heuristics. The intent is to use this result as an input to a higher level reasoning system. Similarly, Huertas, Cole, and Nevatia [6] estimate antiparallel seeds of detected runways, then fill gaps and remove antiparallel segments which correspond to non-runway features. Vasudevan, Cannon, and Bezdek [11] have addressed the problem of partitioning and connecting the roadlike segments extracted by low levels operators (Duda Road Operator). The approach discussed in Medioni and Nevatia [9] is based on relaxation technique to match objects from multi-temporal images. Van Cleynenbreugel, Osinga, Fierens, Suetens, and Oosterlinck [10] use multi-temporal satellite images of the same scene to eliminate transient (vegetation) features. A road segment from one source image is matched to segments in another image using the Dempster-Shafer evidence combination rule.

We present a multiscale algorithm which uses only monospectral image data and some prior highway information (resolution, road width, maximal possible road curvature) to find a highway in a complete satellite scene. The whole scene is first divided into a mosaic of subimages to get a reasonable

Report CS-R9356
ISSN 0169-118X
CWI
P.O. Box 94079, 1090 GB Amsterdam, The Netherlands

optimization size problem. In our case we check the algorithm on SPOT panchromatic images, where these subimages are 320×320 pixels. Single subimages are processed independently and corresponding results are combined together in the last step of the algorithm. The next section deals with several road detection filters. Data compression, described in section 3, is used to lower filter noise, to fill gaps, and to introduce a rough resolution scale for subsequent simplified optimization, described in the section 4. An algorithm for combining single subimage solutions is presented in section 5 and experimental results are presented in section 6.

2. Road detection filters

The purpose of road detection filters is to detect linear elements (possible highways) on a given monospectral high resolution image. An ideal filter should respond only to specified width linear elements with homogeneous pixel grey levels. Because the filter prepares input data for all other data reduction and optimization steps, its optimal design is crucial for a successful road detection algorithm. Eight different filters have been proposed. Their behaviour and speed differ so that they can be used in combination - an approach advocated in [4], or else it is possible to select one which fits best to the image data. Each filter is realized by means of directional masks, whose directions α are denoted using the standard cartographic convention, i.e. N for vertical, NE for diagonal direction, etc. Note that orientation has no meaning, so $N \equiv S, NE \equiv WS$, etc. The number of possible directions is denoted by $\mathcal{A}$. Using more directions provides a better fit to a real road segment. On the other hand, the smaller the angular discretization step is, the longer the mask should be to be able to approximate its direction (only directions N, E, NE, NW are supported by the rectangular pixel lattice). Another disadvantage in this case is the relative increase of the most time consuming part of the algorithm - the filtering and an exponential increase of possible combinations in the final optimization step. A reasonable compromise is to use $\mathcal{A} = 8$ directions for the filtering and to decrease this number to $\mathcal{A} = 4$ in the compression step to simplify subsequent optimization. Let us denote A a set of mask pixels corresponding to a possible linear segment, B a set of off-road pixels on one side of A, and C is a set of off-road pixels on the opposite side of A. The number of conditions tested (or the maximum mask response) is N_c. The Euclidean distance between pixel i and pixel j is denoted d_{ij}. A filter response in the direction α and i-th lattice position is denoted $f(i, \alpha)$. Such a response is evaluated from a mask centered around the i-th lattice pixel. Finally let us denote

$$\delta^*(i, j_1, j_2, \ldots) = \begin{cases} 1 & \text{if } i < j_1 \wedge i < j_2 \wedge \ldots \\ 0 & \text{otherwise} \end{cases} \tag{1}$$

and

$$\delta(B_1, B_2) = \begin{cases} 1 & \text{for } B_1 \subset B_2 \\ 0 & \text{otherwise} \end{cases} . \tag{2}$$

The standard filter can then be specified

$$f(i, \alpha) = \sum_{j=1}^{N_c} \delta^*(|a_j - a_k|, |b_l - a_j|, |c_m - a_k|), \tag{3}$$

where k, l, m are lattice positions such, that

$$d_{jk} = d_{mk} = d_{lj} = d \tag{4}$$

The principle of the mean condition filter is to respond to data only if the mean grey level of the potential road pixels differs by at least 5 % from the mean grey level of the off-road pixels. This condition simulates the human visual discernibility of a linear segment from the background on SPOT images (this threshold was experimentally found from statistical analysis of our data sets). The mean

condition filter responses are defined as follows:

$$f(i,\alpha) = \sum_{j=1}^{N_c}[1-\delta(\mu_B,[0.95\mu_A,1.05\mu_A])]$$

$$[1-\delta(\mu_C,[0.95\mu_A,1.05\mu_A])]\delta^*(|a_j-a_k|,|b_l-a_j|,|c_m-a_k|), \quad (5)$$

together with the equal distance condition (4).

The median condition filter has been motivated by an effort to increase the robustness of the mean condition filter by replacing mean values (μ_A,μ_B,μ_C) with corresponding medians in equation (5).

The T filter is based on the idea of statistical hypotheses testing that the road mean value is equal to the off-road mean value $(H_0 : \mu_A = \mu_B, (\mu_A = \mu_C))$, while the alternative hypothesis is $(H_1 : \mu_A \neq \mu_B, (\mu_A \neq \mu_C))$. We assume that $a_i \in \mathcal{N}(\mu_A,\sigma^2)$, $b_i \in \mathcal{N}(\mu_B,\sigma^2)$, $c_i \in \mathcal{N}(\mu_C,\sigma^2)$, $card(A), card(B), card(C) \geq 2$ and the selections A, B, C are mutually independent. Although it is known that the normality assumption is not valid on most remote sensing data, methods based on this assumption work reasonably well (Bayesian classifier, etc.). β is the predefined probability (chosen by the user) that $\mu_A \neq \mu_B$. The usual choice for β is $\beta = 0.05$ or $\beta = 0.01$. If we denote by $\tilde{\mu}, \tilde{\sigma}^2$ the estimators of mean value and variance of the unknown variables μ, σ^2, respectively (for A,B and C). It can be shown that the random variable T_{AB} defined by:

$$T_{AB} = \frac{\tilde{\mu}_A - \tilde{\mu}_B - (\mu_A - \mu_B)}{[(card(A)-1)\tilde{\sigma}_A^2 + (card(B)-1)\tilde{\sigma}_B^2]^{1/2}}\left[\frac{card(A)card(B)\tilde{f}}{\tilde{f}+2}\right]^{1/2} \quad (6)$$

which gives a measure of distance between $\mu_A - \mu_B$ is a t distribution (Student distribution) [2] with $\tilde{f} = card(A) + card(B) - 2$ degrees of freedom. $t_{\tilde{f}}(\beta)$ defined as follows:

$$P(|T_{AB}| \geq t_{\tilde{f}}(\beta)) = \beta$$

is called the critical value of the t test on the level β. We compare in fact T_{AB} with the critical value and if $|T_{AB}| \geq t_{\tilde{f}}(\beta)$ we consider that μ_A is different from μ_B. β gives the error corresponding to that choice. Similarly we test $H_0 : \mu_A = \mu_C$. Using this test, we can finally specify the T filter as follows:

$$f(i,\alpha) = \sum_{j=1}^{N_c}\delta^*(t_{\tilde{f}}(\beta),|T_{AB}|,|T_{AC}|)\delta^*(|a_j-a_k|,|b_l-a_j|,|c_m-a_k|), \quad (7)$$

together with condition (4).

The idea of the double maxima suppression filter (8) is to suppress filter responses if there are similarly strong responses in more than one direction. We want also to penalize the mutually perpendicular response directions. We denote the maximal response

$$f_1(i,\alpha_1) = \max_{\beta}\{f(i,\beta)\}$$

and the second largest response

$$f_2(i,\alpha_2) = \max_{\beta\neq\alpha_1}\{f(i,\beta)\}.$$

$$f(i,\alpha) = \begin{cases} [1-\frac{f_2(i,\alpha_2)}{f_1(i,\alpha_1)}]\frac{N_c}{|\tan(0.001+\alpha_1-\alpha_2)|} & \text{for } f_2(i,\alpha_2)\neq 0 \text{ and } \alpha=\alpha_1 \\ f_1(i,\alpha_1) & \text{for } f_2(i,\alpha_2)=0 \text{ and } \alpha=\alpha_1 \\ 0 & \text{for } \alpha\neq\alpha_1 \end{cases} \quad (8)$$

The responses $f(i,\beta)$ can be generated for example using the mean condition filter.

The Hadamard filter divides the set A into two mutually disjoint subsets $A = A_0 \cup A_1$ such that $card(A_0) = card(A_1) = card(A)/2$ and the subsequent comparison of grey level mean values of both subsets. We create all divisions such that vectors $\vec{v}_k$ of length $card(A)$ with a single compound v_i representing a subset membership label ($v_i \in \{0, 1\}$) of a corresponding pixel from A, form a base vector set. In the case of $card(A) = 8$ there are 7 possible divisions, for example. The filter output can then be specified as:

$$f(i, \alpha) = \sum_{j=1}^{N_c} \delta^*(|\mu_{A_0,j} - \mu_{A_1,j}|, |\mu_{A_0,j} - \mu_{B,j}|, |\mu_{A_1,j} - \mu_{C,j}|) \tag{9}$$

Where the off-road sets B, C are chosen in such a way that the average city-block distances between all sets

$$\tilde{d}_{A_0,B} = \frac{1}{n} \sum_i \sum_j \tilde{d}_{a_i b_j},$$

$$\tilde{d}_{a_i b_j} = |x_i - x_j| + |y_i - y_j|$$

are as close to each other as possible ($\tilde{d}_{A_0,A_1} \approx \tilde{d}_{A_0,B} \approx \tilde{d}_{A_1,C}$) and n is the number of all possible distances $\tilde{d}_{a_i b_j}$.

The minimum difference variance filter is based on the idea that if the filter mask is exactly located on the road, the variance of grey level difference between road pixels should be smaller than variances in all other remaining directions. If we denote the difference variance estimator in a direction α as

$$\hat{\sigma}^2_{\alpha,\tilde{d}} = \frac{1}{n-1}\left(\sum_{i=1}^{n} |a_i - a_j|^2 - \frac{1}{n}\left(\sum_{i=1}^{n} |a_i - a_j|\right)^2\right) \tag{10}$$

and a_j is a pixel with constant Euclidean distance $\tilde{d}$ in the direction α apart from the pixel a_i and n is the number of all possible such pairs, then we can express this filter as:

$$f_{\tilde{d}}(i, \alpha) = \sum_{j=1}^{N_c} \delta^*(\hat{\sigma}^2_{\alpha,\tilde{d}}, \hat{\sigma}^2_{\beta_1,\tilde{d}}, \hat{\sigma}^2_{\beta_2,\tilde{d}}, \ldots)\delta^*(|a_j - a_k|, |b_l - a_j|, |c_m - a_k|), \tag{11}$$

together with condition (4) and β_i are all remaining directions different from α.

The minimum mean difference filter is based on a similar idea. If the mask direction corresponds to a road element direction then the mean grey level difference between pixels in this direction should be smaller than this variable for all other directions.

$$\hat{\mu}_\alpha = \frac{1}{n} \sum_{i=1}^{n} |a_i - a_j| \tag{12}$$

a_j is again a pixel with constant Euclidean distance $\tilde{d}$ in the direction α apart from the pixel a_i. This filter has the definition given in equation (11) if all $\hat{\sigma}^2$ are replaced with $\hat{\mu}$.

It is not possible to avoid incorrect filter responses introduced by some other linear structures present in an image. These other linear structures differ at least in some of their parameters (length, width, curvature, homogeneity, etc.), so the wrong filter responses introduced by them should be generally weaker than the proper ones. Use of an appropriate filter response threshold can remove some of these cases. Let us assume that all filter N_c conditions are independent of each other, all filter directional responses $f(i, \alpha)$ outside a true road area ($\mathcal{I} - \mathcal{T}$) are also independent, then the final filter result is the maximal response:

$$f(i, \alpha^*) = \max_\alpha \{f(i, \alpha)\} \qquad for \quad \forall i \in \mathcal{I}. \tag{13}$$

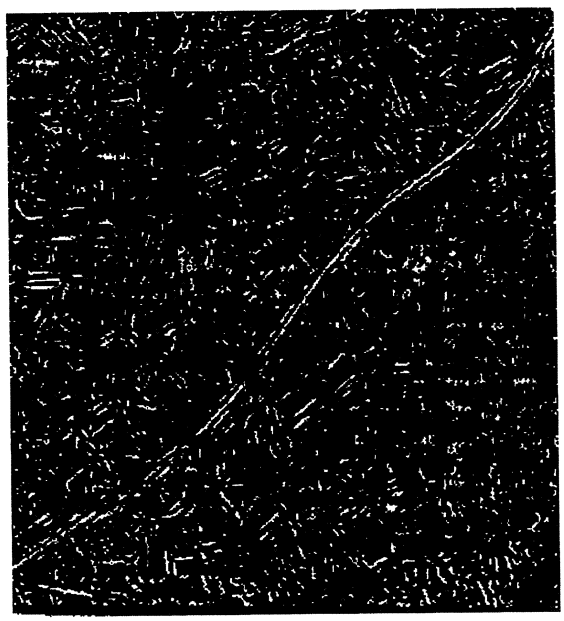

Figure 1: The standard filter output.

If a single direction response of a filter has an additive character of N_c conditions $f_j(i,\alpha)$ (each condition returns 1 if satisfied)

$$f(i,\alpha) = \sum_{j=1}^{N_c} f_j(i,\alpha) \tag{14}$$

and we assume the probability of an elementary off-road incorrect reaction

$$P_o = P(f_j(i,\alpha) = 1 | i \in (\mathcal{I} - \mathcal{T})) \tag{15}$$

equal for $\forall i, j, \alpha$, then the probability of the off-road incorrect response has the binomial distribution.

$$P(f(i,\alpha^*) \geq t | i \in (\mathcal{I} - \mathcal{T})) =$$

$$\sum_{\alpha} P(f(i,\alpha) \geq t | i \in (\mathcal{I} - \mathcal{T})) = \mathcal{A} \sum_{j=t}^{N_c} \binom{N_c}{j} P_o^j (1 - P_o)^{N_c - j} \tag{16}$$

We require the probability of error to be smaller than a specified value β

$$P(f(i,\alpha^*) \geq t | i \in (\mathcal{I} - \mathcal{T})) \leq \beta. \tag{17}$$

From this inequality we can specify the threshold t. The probability P_o (see equation (15)) can be estimated experimentally or we can find its value analytically for the standard filter. Experimental estimation is based on equation (16) and on the fact that

$$P(f(i,\alpha^*) \geq \tilde{t} | i \in (\mathcal{I} - \mathcal{T})) \doteq \frac{card(\mathcal{F} \cap (\mathcal{I} - \mathcal{T}))}{card(\mathcal{I})} \tag{18}$$

for some $\tilde{t}$, where $\mathcal{F} = \{f(i,\alpha^*) : f(i,\alpha^*) \geq \tilde{t}\}$.

Comparing different filter outputs (Figs. 1 and 2), it is possible to see (visually as well as using statistical criteria - to be described in a following paper) differences in their behaviour. The standard

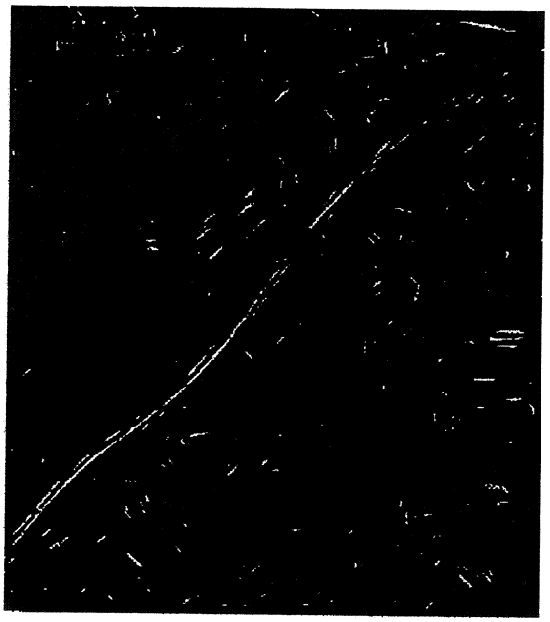

Figure 2: The mean condition filter output.

filter is the most noisy one. The Hadamard filter is only slightly better but is computationally more demanding. Similarly we have not seen a significant improvement in the median condition filter behaviour compared to the mean condition filter to advocate its increased computational complexity. Our experiments reveal the mean condition filter to be the fastest one, since the time consuming absolute difference evaluation is done only if the mean condition is satisfied. The signal to noise ratio was also found to be the best for this filter, but there is also room for improvement of the T filter performance by improved tuning. Finally, another improvement can be reached by combining the double maxima suppression principle with the mean condition filter. The mean condition filter appears to provide a practical compromise between filter robustness and computational complexity.

3. Data compression

Statistical data analysis of road and off-road image segments reveals the difficulty to design a noise-free road detection filter. Any filter inevitably will generate some incorrect responses due to low separability of road and off-road data. Another source of incorrect filter responses stems from the presence of linear artifacts with similar parameters to recognized highways, such as, rivers, side roads, runways etc. Optimization in the original fine resolution scale is a time consuming task which is complicated by the presence of incorrect filter responses or the lack of any response (gaps located in an actual highway side). A reasonable solution is to apply some sort of low-pass filter technique and to change the resolution scale. The data compression is done using the Hough transformations for pairs of rough scale new pixels in four principal road directions (horizontal, vertical and both diagonals). Single local Hough transformations

$$\xi = (y - y_0)\cos\theta - (x - x_0)\sin\theta \tag{19}$$

have not only the desired low-pass filter and gap filling properties, but can also be evaluated very quickly due to the reduced amount of data (two rough pixels) involved. An element (θ, ξ) of the Hough transformation accumulator array is incremented by a corresponding $f(i, \alpha^*)$. From every local directional Hough transformation we select the weight of the most probable line (Fig. 3) as a

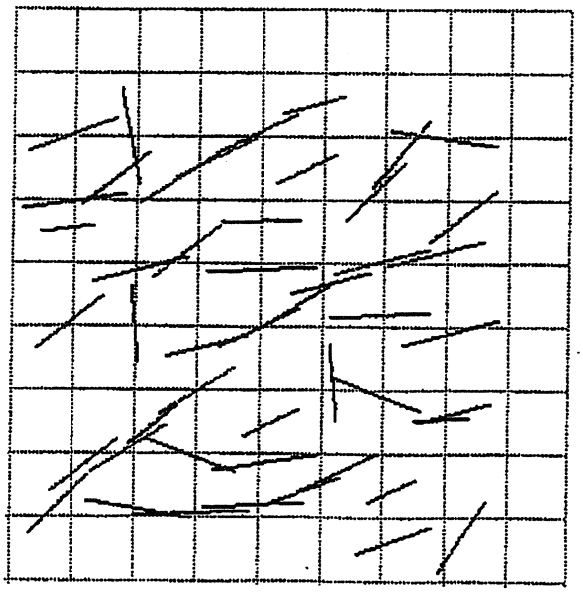

Figure 3: The Hough transformations for diagonal pairs.

local representative of our trust in a highway crossing between two corresponding rough scale pixels. This weight is modified according the angular difference between the line found angle (θ) and the angle of the pair of rough pixels (η) processed

$$v = \tilde{v}|\cos(\theta + \eta)| \tag{20}$$

The result is a dual lattice of all possible crossings between rough scale pixels.

4. Optimization

The optimization task attempts to find an optimal path through the dual lattice over the rough scale resolution image. We assume the presence of just one highway in a processed image. (The removal of this restriction is discussed in the concluding section.) The image to be processed is limited to the width corresponding to 7 dual lattice row elements, each with four possible basic directions. This restriction gives a reasonable number of possible combinations. These possible lattice row configurations are precomputed and stored in a dictionary. Necessary geometrical restrictions (maximal possible road curvature) are incorporated through the selection of possible successive lattice row configurations stored for each row configuration. Let us denote the dual lattice S, single sites s and a binary array over S denoting the presence or absence of a road element $U = (u_s, s \in S)$. The corresponding Hough transformation array is $V = (v_s, s \in S)$. The optimality criterion selected is the mean response per lattice element:

$$F(U,V) = \frac{\sum_{s\in S} u_s v_s}{\sum_{s\in S} u_s} \tag{21}$$

$$\hat{U} = \arg\max_U F(U,V). \tag{22}$$

The function (21) is nonlinear and cannot be directly solved using dynamic programming techniques. Let us define a sequence of $\lambda_i, i = 0, 1, \ldots$:

$$\lambda_{i+1} = F(U^i, V) \tag{23}$$

with some arbitrary λ_0 and

$$\phi(U, V, \lambda) = \sum_{s \in S} u_s(\lambda - v_s) \tag{24}$$

where

$$U^i = \arg\min \phi(U, V, \lambda_i). \tag{25}$$

Then it can be shown [7] that

$$\hat{U} = \lim_i \lambda_i. \tag{26}$$

This optimization problem can be solved using iterative dynamic programming. Practical realization in our case usually needs only few iterative steps (3-5) to find an optimal path. Once an optimal rough scale road has been determined, it can be used as the guidance pattern for the final original scale road location algorithm. This precise localization is done using the A^* algorithm [3]. The algorithm always ends with a proposed road even if no road is present in a tested subimage. This problem can be handled by checking filter values in suspected road locations. The criterion used is the mean difference from the optimal filter response

$$\mathcal{D} = f_{\max} - \frac{1}{n} \sum_{i=1}^{n} f(i, \alpha^*) \tag{27}$$

(its value can be obtained from the A^* algorithm). The mean road filter response should be greater or equal to the threshold t (17) so a subimage road must be rejected if its $\mathcal{D} > f_{\max} - t$.

5. Large image processing

Due to the sharp increase in the number of possible configurations with the increase of dual lattice row width, we are limited in image optimization up to 7 dual lattice boxes. The corresponding image maximal width depends on satellite image resolution and highway parameters. To process a large satellite image or a mosaic of such images we have to divide such a scene into individual subscenes which are independently processed. Combining single individual results into a final mosaic can sometimes lead to a desired solution. But in some more difficult cases (large urban areas, rivers or rail tracks having similar geometric properties with highways) we can endup with a mosaic where some part of a highway is missing or some subimage has an incorrect solution. To solve these cases we use the following strategy based on border crossing points.

Every subimage can have 0 or 2 border crossing points . A border crossing point i is assumed to be reliable if it is common for two neighbouring subimage roads and the road curvature in this crossing point i fulfills the maximal road curvature limitation, then the weight of this point is set to $\gamma_i = 2$. If there is no continuation from point i in one subimage or the i point does not fulfill the curvature condition, its weight is set to one ($\gamma_i = 1$). $\gamma_i = 0$ is the weight of a crossing point on the outer border of the whole large image. The longest found road segment ($\max \sum_i \gamma_i$) is followed until the point j with $\gamma_j = 1$. The optimization step is repeated in neighbouring subimage forcing the start of dynamic programming in a dual lattice point corresponding to point j in fine scale resolution . This new segment, forced to bind with the previously found long road segment, can violate the maximal curvature limit in the crossing point j or can end in a point l with $\gamma_l = 1$. Such cases are caused by the tendency of the optimization algorithm to connect together part of the road with a strong noise-introduced response (i.e. river). Such areas can be detected by tracking filter responses corresponding to the optimization result (monitoring changes in $\mathcal{D}$). The optimization algorithm is

Figure 4: Toulouse 1.

enforced to keep the maximal highway curvature limitation in its solution and therefore inevitably introduces an inhomogeneous part between two parts of a proposed solution supported by different courses. This case is solved by erasing data in the Hough transformation accumulator arrays which supports the incorrect part of a solution and running the subimage optimization part on a restricted data set once more.

6. Results

The example on Fig. 4 shows SPOT panchromatic scene from the vicinity of Toulouse. By just combining single subimage results we obtained the proper solution (Fig. 5) which is easily detected by the road tracking algorithm described in the previous section. All detected road crossing points have value $\gamma_i = 2$ except both outer border points. Results from subimages 11,32,41,42 and 43 were rejected by the criterion (27). Result 14 corresponds to the side branch of a detected highway, results 22 and 32 correspond to a dual-carriage way. Solutions 21 and 31 were combined by the algorithm from several smaller responses.

While the first example did not require any further processing, the second scene from the vicinity of Toulouse (Fig. 6) is our most complicated example because it contains lot of linear structures with similar parameters to the detected highway.

Fig. 7 shows the resulting mosaic using the standard Hough transformation in the compression step. The proper results appear only in subimages 12 and 22. The lower part of subimage 43 is also correct. Using the modified Hough transformation (20) always improves our results, in this example additional correct result in the subimage 33 was obtained. The result 43 was automatically corrected using the fixed start (to bind the 33 result) dynamic programming technique from the previous section, but

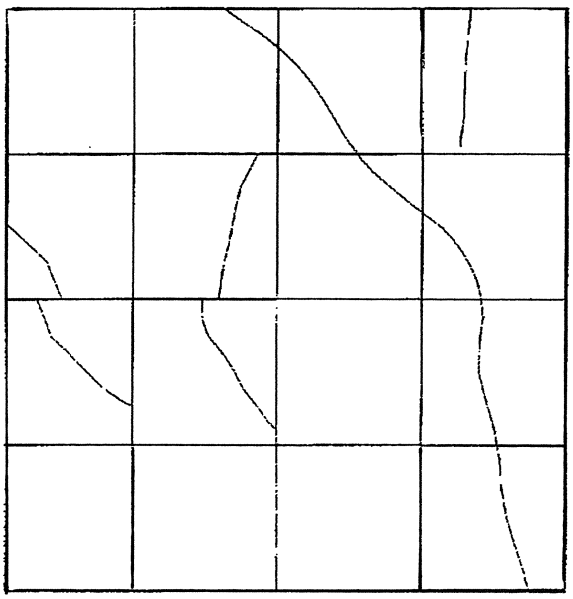

Figure 5: Toulouse 1: detected highway.

Figure 6: Toulouse 2.

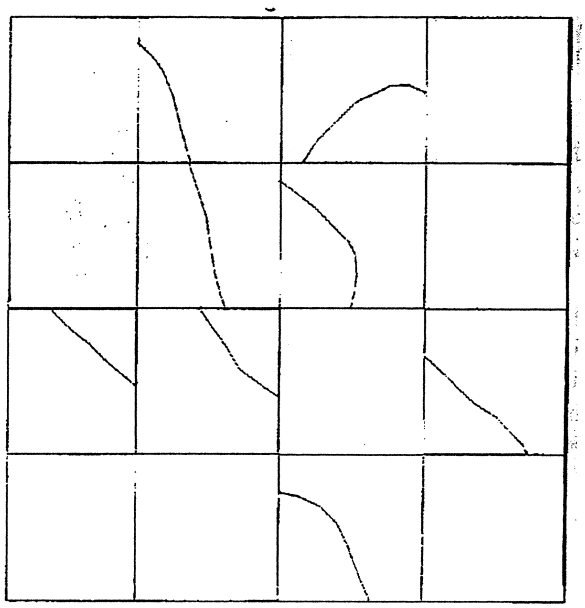

Figure 7: Toulouse 2 (standard Hough tr.).

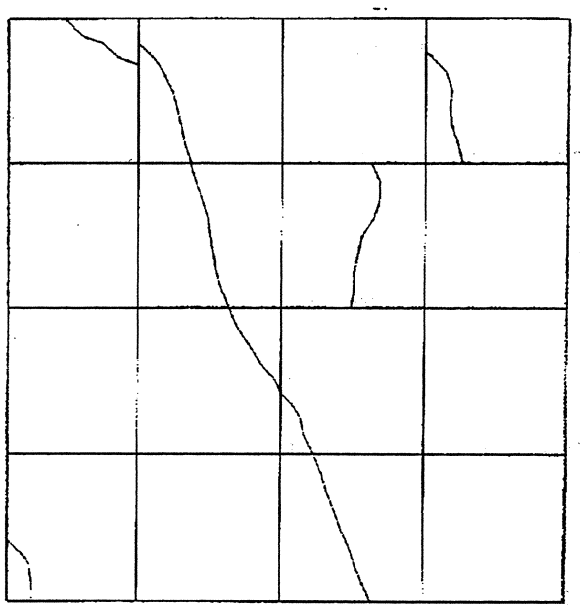

Figure 8: Toulouse 2: final result.

this technique fails on two remaining undesired results 11 and 32. The true highway in the subimage 11 lies in a border area unprocessed in the rough scale optimization and can be solved by subimage overlapping or a modification of the A^* algorithm. The subimage 32 also contains a river with highway-like parameters and has stronger filter response than the highway itself. The algorithm was not able to combine both large road segments through the subimage 32 trying to enforce the dynamic programming starting points on ends of these highway segments. The algorithm therefore removed data supporting this unsatisfactory solution and run the optimization step once more with the proper solution as a result. Fig. 8 shows the final result of the algorithm (the subimage overlapping was not yet implemented).

7. CONCLUSION

The algorithm described in this paper has been checked against several panchromatic SPOT images from the vicinity of Toulouse and La Rochelle with encouraging results. Correct highway recognition has been achieved, in several cases, by just connecting single subimage results. Other cases were solved using enforced dynamic programming and data elimination techniques (Fig. 8). Another possible solution we are currently investigating is combining the local (subimage) optimization technique with the global one (two resolution optimization). Our algorithm can be modified to detect other linear structures in images such as rivers or rail tracks. Using the data elimination technique described the recognition of multiple highways present in processed remote sensing data can be solved as well.

REFERENCES

1. Z. Aviad, P.D. Carnine, " Road finding for road-network extraction," in *Computer Soc. Conf. on Computer Vision and Pattern Recognition,* Ann Arbor, pp. 814-819, 1988.
2. A. Bendat, D. Piersol, *Random Data: Analysis and Measurement Procedures,* Wiley Interscience, 1971.
3. R.O. Duda, P.E. Hart, *Pattern Classification and Scene Analysis,* Wiley, New York, 1973.
4. M.A. Fischler, J.M. Tenenbaum, H.C. Wolf, " Detection of roads and Linear Structures in Low-Resolution Aerial Imagery Using a Multisource Knowledge Integration Technique," *Computer Graphics and Image Processing,* Vol. CVGIP–15, pp. 201-223, 1981.
5. R.M. Haralick, J.B. Campbell, S. Wang, " Automatic Inference of Elevation and Drainage Models from a Satellite Image," *Proc. IEEE* , Vol. 73, pp. 1040-1053, 1985.
6. A. Huertas, W. Cole, R. Nevatia, " Detecting Runways in Aerial Images," in *Image Understanding Workshop,* Los Angeles, pp. 272-305, 1987.
7. B. Jedynak, D. Geman, A. Gagalowicz, " Detection de Reseaux Routiers a partir des images du Satellite in SPOT," in *8 Congres Reconnaissance des Formes et Intelligence Artificielle,* Vol. 1, pp. 489-497, 1991.
8. D.M. McKeown, J.L. Denlinger, " Cooperative methods for road tracking in aerial imagery," in *Computer Soc. Conf. on Computer Vision and Pattern Recognition,* Ann Arbor, pp. 662-672, 1988.
9. G. Medioni, R. Nevatia, " Matching Images Using Linear Features," *IEEE Trans. PAMI* , Vol. 6, pp. 675-685, 1884.
10. J. Van Cleynenbreugel, S.A. Osinga, F. Fierens, P. Suetens, A. Oosterlinck, " Road extraction from multi-temporal satellite images by an evidential reasoning approach," *Pattern Recognition Letters* , Vol. 12, pp. 371-380, 1991.
11. S. Vasudevan, R.L. Cannon, J.C. Bezdek, " Heuristics for Intermediate Level Road Finding Algorithms," *Computer Vision, Graphics and Image Processing,* Vol. CVGIP–44, pp. 175-190, 1988.
12. M. Zhu, P. Yeh, " Automatic Road Network Detection on Aerial Photographs," Rep. CAR-TR-177, Center for Automation Research, University of Maryland, MD, 1986.